

Pairing Amplitude Fluctuations in High Temperature Superconductors

Philippe Curty¹ and Hans Beck²

¹*The Abdus Salam International Centre for Theoretical Physics, 34014 Trieste, Italy*

²*Université de Neuchâtel, 2000 Neuchâtel, Switzerland*

(Dated: March 15, 2005)

In a previous letter we have shown that amplitude fluctuations are responsible together with phase fluctuations for the pseudogap phenomena in high temperature superconductors. Here we present the more detailed theory of the amplitude and phase fluctuations approach in the framework of a fermionic pairing model. New experimental comparisons are presented for the specific heat of the cuprate LSCO confirming the generality of the approach. The decrease of amplitude fluctuations near optimal doping create the illusion of a quantum critical point which in fact does not exist.

One major problem concerning high temperature superconductors is to establish the correct phase diagram temperature versus hole or electron doping. A related question is the interpretation of the anomalous behaviour above the critical temperature. This regime is called pseudogap [1, 2] because it contains effects similar to superconductivity like a partial suppression of electronic density of states. The pseudogap region starts below a temperature T^* where observable quantities deviate from Fermi liquid behaviour and seems to be present well inside the superconducting phase.

Until now two interpretations seem to emerge: the first point of view assumes the existence of quantum critical point (QCP) sitting in the middle of the superconducting regime [3]. This quantum critical point is due to an (unknown) order parameter which is competition with superconductivity. The experimental evidences for a QCP are however not convincing until now. Moreover effects of quantum fluctuations are suppressed by superconductivity at low temperature. Loram and Tallon [4] have analyzed many experimental data like specific heat or scanning tunneling experiments and extract the value of an external energy scale E_g . In their analysis, they assume the presence of an external gap and extract its value by fitting experiments.

The second group of approaches tends to analyse the consequence of pairing and superconductivity on the phase diagram [5, 6, 7]. The pseudogap phase is then due to precursor effects of superconductivity or amplitude pairing fluctuations for example. With this point of view, one does not need the existence of the QCP. However, there is still the need to explain the characteristic pseudogap energy found E_g by Loram and Tallon [4].

It is perhaps important to remind that T^* is a crossover temperature that can be directly seen in experiments where observable quantities deviate from Fermi liquid behaviour. E_g in the sense of ref. [4] is a phenomenological energy scale extracted by fitting experiments according to a simple theory of gapped electrons.

In a recent letter [7], the importance of treating both amplitude and phase fluctuations in a pairing model has been shown. Using this method, it is possible to fit accurately experiments and to extract all the phase diagram of cuprates except the antiferromagnetic regime. By expanding observables around the average amplitude,

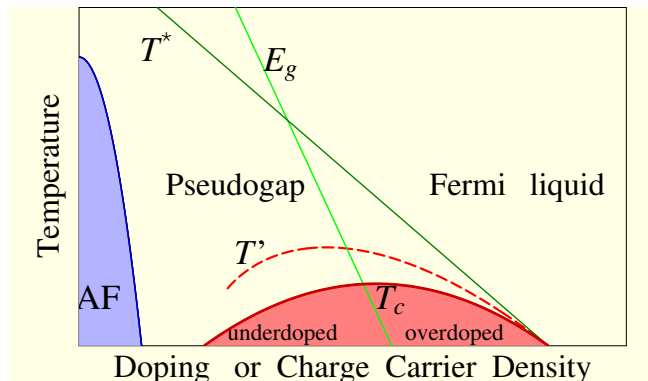


FIG. 1: Schematic experimental phase diagram of cuprates. The pseudogap region of the copper oxides phase diagram lies between the critical temperature T_c and a temperature T^* that interpolates the antiferromagnetic domain noted by AF. The temperature T' has been reported in several experiments [8]. The energy scale E_g has also been found in many experiments like specific heat [4].

one can compute thermodynamic quantities like specific heat or magnetic spin susceptibility. Two temperature regions have to be distinguished (see Fig. ??): for a relatively small temperature interval $T_c < T < T_\phi$ the phase of ψ is still correlated in space over some coherence length ξ (the Kosterlitz-Thouless coherence length in $2d$). Thus, in this regime, observables are governed by correlated phase fluctuations described by the XY-model. For $T_\phi < T < T^*$, phases of ψ are essentially uncorrelated (ξ is on the order of the lattice constant), but $|\psi|$ is still fluctuating and non-zero, signaling local pair fluctuations. This explains the wide hump between T_c and temperature T^* seen in specific heat experiments [1], the depression of the spin susceptibility [9] and the persistence of the pseudogap for $T < T^*$.

One important result is the extracted phase diagram: by fitting the experiments it is possible to get the phase stiffness V_0 , the mean-field temperature T_0 and the energy scale E_g versus doping.

In this paper, we will show that the phase diagram of cuprates has indeed an energy scale E_g similar to the one found in [4]. However this pseudogap energy scale is

due the presence of a pairing attraction and controlled by amplitude fluctuations. When these two effects are taken into account, they produced a very large E_g in the underdoped regime where the superfluid density is low and fluctuations are large. In the maximum T_c regime, E_g becomes rapidly small because amplitude fluctuations decrease rapidly. The interaction strength is also decreasing when overdoping. This creates the illusion of a QCP in the middle of the superconducting region.

Our approach has the advantage that the only strong assumption is that high temperature superconductivity is caused by a fermionic pairing attraction which seems to be likely the case. All other assumptions are only technical and related to the calculations.

Various experimental observations can indeed be interpreted in terms of fluctuations of the pairing field $\psi = |\psi|e^{i\phi}$, and that two temperature regions have to be distinguished (see Fig. 1): for a relatively small temperature interval $T_c < T < T_\phi$ the phase of ψ is still correlated in space over some coherence length ξ (the Kosterlitz-Thouless coherence length in $2d$) whereas the amplitude $|\psi|$ is almost constant. Thus, in this regime, observables are governed by correlated phase fluctuations described by the XY-model. For $T_\phi < T < T^*$, phases of ψ are essentially uncorrelated (ξ is on the order of the lattice constant), but $|\psi|$ is still non-zero, signaling independent fluctuating local pairs. This explains the wide hump seen in specific heat experiments [1], the depression of the spin susceptibility [9] and the persistence of the pseudogap for $T < T^*$. Moreover, a magnetic field that destroys this pseudogap has to break fluctuating pairs and must therefore be much higher than the one which suppresses phase coherence and thus superconductivity [10].

Our approach has a major difference with the Emery and Kivelson phase fluctuations scenario [5] of the pseudogap regime: our calculations show that phase fluctuations influence the pseudogap only up to a temperature T_ϕ which is much smaller than T^* . Above T_ϕ , observables are thus only determined by the amplitude of the pairing field.

The existence of a temperature intermediate between T_c and T^* has also been mentioned by Devillard and Ranninger [11]: using a Boson-Fermion description of pairing in cuprates, they find that uncorrelated pairing of electrons leads to the opening of a pseudogap at T^* . These pairs acquire well behaved itinerant features at T_B^* , leading to partial Meissner screening, and thus to diamagnetic susceptibility, and Drude-type behaviour of the optical conductivity. As a function of lattice anisotropy (and thus of doping) T_B^* has the same tendency as T_c , whereas the higher temperature T^* has the opposite trend. Although in ref [11] T_B^* is related to the temperature where the pair life time becomes long, it could be identified with our T_ϕ .

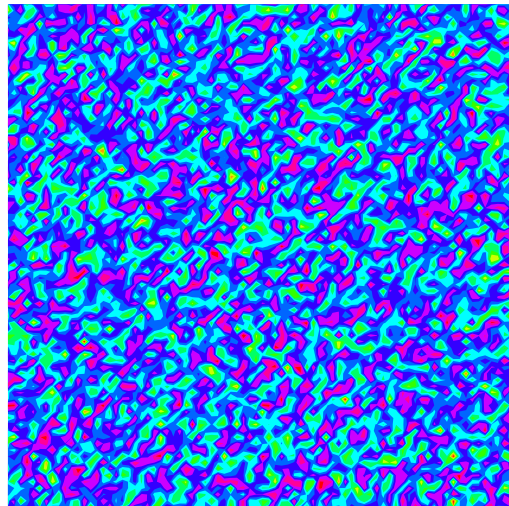


FIG. 2: Amplitude of the pairing field above T_c on a 80×80 array by cluster Monte Carlo simulations: dark is for large amplitude and hell for low amplitude.

I. MODEL AND EFFECTIVE ACTION

We are not interested at the origin of pairing between electrons but at the consequences of pairing on the phase diagram or the physical quantity like specific heat. Hence we assume that there is an attractive force between fermions, and we base our calculations on a d -wave attractive Hubbard model

$$H = - \sum_{\langle i,j \rangle \sigma} t c_{i\sigma}^\dagger c_{j\sigma} - U \sum_i Q_d^\dagger(i) Q_d(i) \quad (1)$$

with a hopping t between nearest neighbour sites i and j on a square lattice. The interaction favours the formation of onsite d -wave pairs since

$$Q_d^\dagger(i) = \sum_j D_{ij} Q_{ij}^\dagger \quad (2)$$

where $D_{ij} = 1, (-1)$ for i being the nearest neighbour site of j in horizontal (vertical) direction.

$$Q_{ij}^\dagger = \left(c_{i\uparrow}^\dagger c_{j\downarrow}^\dagger - c_{i\downarrow}^\dagger c_{j\uparrow}^\dagger \right) / \sqrt{2} \quad (3)$$

is an operator creating a singlet pair on neighbouring sites. Decoupling the interaction with the help of a Stratonovich-Hubbard transformation, the partition function $Z = \text{Tr} e^{-\beta H}$ is then

$$Z = Z_n \int D^2\psi \left\langle \mathcal{T} e^{-\int_0^\beta d\tau \sum_i \left(\frac{1}{\nu} |\psi|^2 + \psi Q_d^\dagger(i) + \text{hc} \right)} \right\rangle_{H_n}$$

where

$$\psi = \psi(i, \tau) = |\psi(i, \tau)| e^{i\phi(i, \tau)}, \quad (4)$$

and $H_n = -\sum_{\langle i,j \rangle \sigma} t c_{i\sigma}^\dagger c_{j\sigma}$ is the non-interacting part. The trace over the fermionic operators can be evaluated yielding

$$Z = \int D^2\psi e^{-\int_0^\beta d\tau [\sum_i \frac{1}{\tau} |\psi|^2 + \text{Tr} \ln G]}. \quad (5)$$

Here G is a Nambu matrix of one-electron Green functions for fermions interacting with a given, space and time dependent pairing field $\psi(i, \tau)$. The Green functions are solution of Gorkov's equations (see [12]).

Expanding (5) in power of $\vec{\nabla}\psi$, Z can be written as a functional integral involving an action $S[\psi]$ for a field ψ that changes slowly in space and that can be taken time-independent:

$$S[\psi] = S_0(|\psi|) + S_1(\vec{\nabla}\psi) \quad (6)$$

where S_0 is a local functional of ψ :

$$S_0(|\psi|) = V \frac{|\psi|^2}{U} - \frac{2}{\beta} \sum_q \log[2 \cosh \beta E_q/2] \quad (7)$$

and $S_1 = c \int d^3r |\vec{\nabla}\psi|^2/2$ can be considered as the deformation or kinetic energy where c is a constant. The quasi-particle energy is $E_q = \sqrt{|\psi|^2 + (\varepsilon_q - \mu)^2}$.

Now we would like to compute thermodynamic observables such as energy $U = \langle S \rangle_S$, specific heat and spin susceptibility. The point is that we want to keep the XY universality class of the transition together with the fermionic character of the system: in the limit of high density or weak interaction, the superconductor should be described by a BCS like mean field theory whereas in the low density limit with strong interaction the transition becomes XY like. Our goal is to derive a theory that describes these two regimes and, of course, the intermediate regime.

Our main strategy will be to neglect amplitude correlations since simulations show that they are weak between different sites i, j : $\langle |\psi|_i |\psi|_j \rangle - \langle |\psi|^2 \rangle \approx 0$ since the amplitude is always positive and cannot show any critical behaviour. In this spirit, two different approaches are possible:

First approach: the amplitude is fixed but still temperature dependent, and is determined by a suitable variational equation. Fluctuations from the XY model are kept as well as the amplitude weight coming from the Jacobian of the cartesian to polar coordinates transformation.

Second approach: the energy is expanded around the average amplitude. Higher powers of amplitude fluctuations are neglected. Here the local coupling between phase and amplitude is kept, and amplitude are allowed to fluctuate.

II. VARIATIONAL METHOD

The integration of the partition function can be expressed in polar coordinates using the transformation:

$$D\psi = \prod_i \int_{-\infty}^{+\infty} d\psi_i d\psi_i^* = \prod_i \int_0^{+\infty} d|\psi_i| |\psi_i| \int_0^{2\pi} d\phi_i \quad (8)$$

Rewriting the free energy F in terms of a constant amplitude $|\psi|$ yields

$$F = -\frac{1}{\beta} \log \int D\phi e^{-\beta(S_0(|\psi|) - \log(|\psi|)V/\beta + S_1)}$$

where the Jacobian $|\psi_i|$ of the polar transformation is put into the exponential, and V is the volume. Taking the derivative of F with respect to $|\psi|$ and equating it to zero leads to the self-consistent equation:

$$\frac{\partial S_0(|\psi|)}{\partial |\psi|} - \frac{V}{\beta |\psi|} + c |\psi| \langle |\vec{\nabla} e^{i\phi}|^2 \rangle_{S_1} = 0. \quad (9)$$

Evaluating equation (9) and multiplying it with $|\psi|/2$

$$\frac{|\psi|^2}{U} - \frac{|\psi|^2}{W} \int_{-\mu}^{W-\mu} d\xi \frac{\tanh\left(\sqrt{\xi^2 + |\psi_k|^2}/(2T)\right)}{\sqrt{\xi^2 + |\psi_k|^2}} - \frac{1}{2\beta} + c |\psi|^2 \langle |\vec{\nabla} e^{i\phi}|^2 \rangle_{S_1} = 0. \quad (10)$$

The first term, called the amplitude contribution, leads to the BCS gap equation if other contributions are neglected. The second comes from the Jacobian and implies that the amplitude is never zero. The third term is the expectation value of the energy U_{xy} in the XY model with a constant dimensionless coupling K

$$K = \frac{V_0}{T} \frac{|\psi|^2}{|\psi_0|^2}. \quad (11)$$

where V_0 is the zero temperature phase stiffness, and $|\psi_0|$ is the zero temperature amplitude. This contribution characterises the influence of the phase fluctuations. $U_{xy}(K)$ is a monotonic decreasing function with an inflexion point at T_c . Solutions of equation (10) are reliable for all temperatures except for $T \ll T_c$. However they are only expected to be accurate at T_c if the average amplitude is large and not varying too much with temperature.

III. AVERAGE VALUE METHOD

Since simulations show that amplitude correlations are weak, we can expand the energy around the average amplitude where it is not coupled to the phase. The energy is then

$$U = \langle S \rangle_S \approx S_0(\langle |\psi| \rangle) + \langle S_1 \rangle_S \quad (12)$$

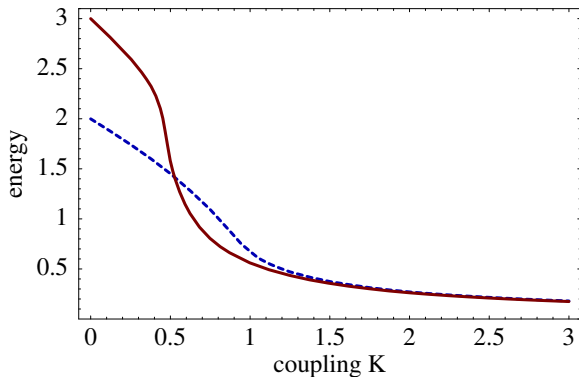


FIG. 3: Dimensionless energy of the XY model as a function of the coupling K defined in equation (11). The continuous line is for 3 dimensions and dashed is for 2 dimensions. Note that the phase transition occurs near the cusps.

Here, $S_0(\langle|\psi|\rangle)$ is the first term of an expansion of the average $\langle S_0(|\psi|\rangle)$ around $\langle|\psi|\rangle$.

$$\begin{aligned} \langle S \rangle_S &= \left\langle S_0(\langle|\psi|\rangle) + c_1(|\psi| - \langle|\psi|\rangle) + c_2 \frac{(|\psi| - \langle|\psi|\rangle)^2}{2} + \dots \right\rangle \\ &= S_0(\langle|\psi|\rangle) + \sum_{n=1}^{\infty} \frac{c_n}{n!} \langle (|\psi| - \langle|\psi|\rangle)^{2n} \rangle \\ &= S_0(\langle|\psi|\rangle) + \sum_{n=1}^{\infty} c_n \frac{(2n+1)!!}{n!} (\langle|\psi|^2\rangle - \langle|\psi|\rangle^2)^n \end{aligned} \quad (13)$$

since amplitude fluctuations around their average value can be considered as gaussian. Higher corrections term are proportionnal to powers of the square of the standard deviation $\langle|\psi|^2\rangle - \langle|\psi|\rangle^2$. Although amplitude fluctuations are large, the standard deviation is half of the average amplitude, powers of $\langle|\psi|^2\rangle - \langle|\psi|\rangle^2$ are very small compared to the average amplitude itself. This is why we only take the first term of the expansion which already yield the interesting physics. Additional terms would just add more fluctuations.

For simplicity, averages are computed using a normalised Ginzburg-Landau action S_{GL} (see [13]) whose potential part U_{GL} is equal to the first two terms of the expansion of S_0 with respect to $\beta|\psi|$:

$$S_{GL}[\psi] = k_B V_0 \int d^3r (U_{GL} + S_1) \quad (14)$$

where

$$U_{GL} = \eta^2 (t|\tilde{\psi}|^2 + \frac{1}{2}|\tilde{\psi}|^4), \quad (15)$$

and $t \approx T/T_0 - 1$ is the reduced temperature, $\tilde{\psi} = \psi/|\psi(T=0)|$ is the reduced field, T_0 is the mean field BCS pairing temperature. S_{GL} is normalised with a lattice spacing ε .

$$\eta := \varepsilon/\xi_0,$$

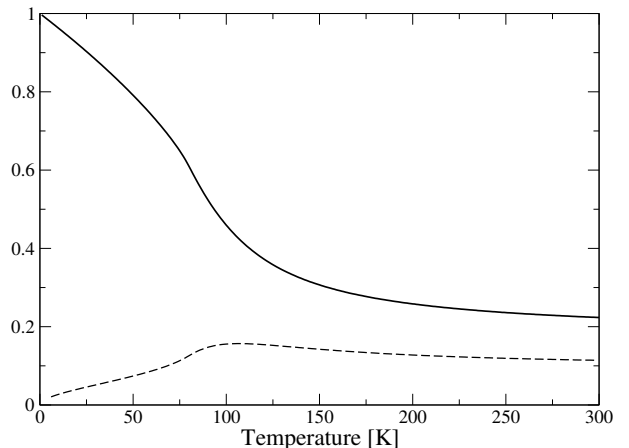


FIG. 4: Average amplitude (thick line) and the corresponding standard deviation (dashed line). Parameters are $V_0 = 215$, $T_0 = 140$. Note that T_c is about 80K whereas the amplitude remains non zero at least up to 300K.

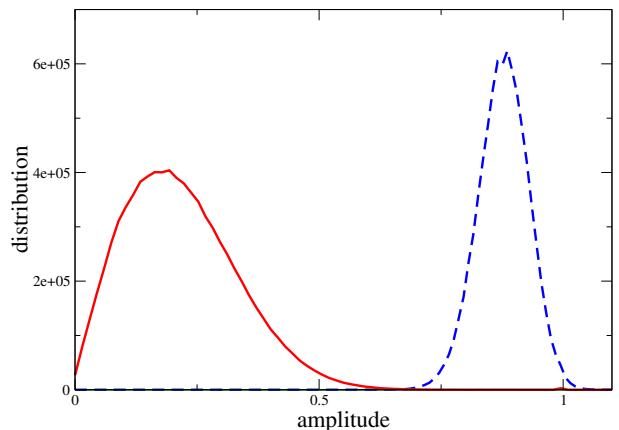


FIG. 5: Amplitude distribution for $T = 300\text{K}$ (thick line) and $T = 30\text{K}$ (dashed line). Parameters are $V_0 = 215\text{K}$, $T_0 = 140\text{K}$. Note the broadening of the amplitude distribution at high temperature, i.e the increase of fluctuations, compared to the low temperature distribution where the distribution is narrower.

where ξ_0 is the mean field coherence length at zero temperature, and V_0 is the zero temperature phase stiffness. Contrary to the variational method, amplitude and phase are still *locally* coupled through S_1 . The energy becomes

$$U \approx S_0(\langle|\psi|\rangle_{GL}) + \langle S_1 \rangle_{GL} \quad (16)$$

where

$$S_0(\langle|\psi\rangle) = (V \langle|\psi\rangle^2/U) - \frac{2}{\beta} \sum_q \log[2 \cosh \beta E_q/2]$$

corresponds the BCS free energy for which the gap value is determined by the GL average. The quasi-particle energy is $E_q = [(\varepsilon_q - \mu)^2 + \langle|\psi\rangle^2 \cos^2(2\theta)]^{1/2}$ where μ is the chemical potential. The d -wave symmetry manifests itself by the angle dependent amplitude $|\psi| \cos(2\theta)$ where θ is the angle in k space with respect to k_x direction.

The value of η depends on the coarse-graining procedure and is fixed for each sample. Observables are not very sensitive to changes in η .

Both approaches are valid below and above the critical temperature T_c which is the temperature where the phase stiffness becomes zero. However the average value method gives good results for all values of T_0 and V_0 whereas the variational method works better in the underdoped regime, i.e. for $V_0 < T_0$.

It is important to notice that the amplitude is fluctuating although it is fixed to its averaged value in observables. In figure 4, the average amplitude and its standard deviation are shown. One can note that the latter is approximately half of the averaged amplitude. Since the amplitude distribution around its average value is almost gaussian, the probability density $p(|\psi|)$ has the following form:

$$p(|\psi|) \approx e^{-\frac{(|\psi| - \langle|\psi\rangle)^2}{\langle|\psi\rangle^2}} \quad (17)$$

This means that the amplitude has values ranging from 0 to $2\langle|\psi\rangle$ causing the large average value $\langle|\psi\rangle$.

Computer simulations of the statistical ensemble $\{\psi\}$ under the action S_{GL} have been done using a standard Monte Carlo procedure to update amplitude $|\psi|$ and a Wolff [14] algorithm for the phase ϕ in the same way as for the real Φ^4 model [15]. Typically 10^4 sweeps are needed to obtain good statistics.

Since the fitting procedure is done completely automatically, one has to simulate first the Ginzburg-Landau action (??) for all possible parameters a and b . Once a mesh of simulations has been done, it is possible to interpolate the surface defined by $\langle|\psi\rangle(a, b)$ and to have access all values of $\langle|\psi\rangle(a, b)$. The same is done for the energy $\langle|\nabla\psi|^2\rangle(a, b)$

IV. SPECIFIC HEAT

In both approaches, the specific heat C is the sum of the amplitude C_0 and the gradient C_1 contributions. Defining the reduced specific heat $\gamma = C/(\gamma_n T)$, we have

$$\gamma = \gamma_0 + \gamma_1 \quad (18)$$

where γ_1 is divided by T_c instead of T since S_1 is classical and does not satisfy the third law of thermodynamic.

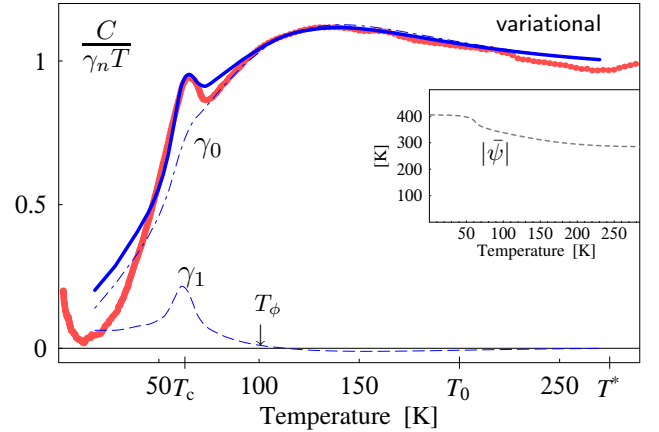


FIG. 6: The reduced specific heat γ from the variational method (thick), which is the sum of the gradient γ_1 (dashed) and amplitude γ_0 (dotted-dashed) contributions, reproduces measurements of $\text{YBa}_2\text{Cu}_3\text{O}_{6.73}$ (points). *Inset:* The dashed line is the temperature dependent amplitude $|\bar{\psi}|$ from equation (10).

The amplitude contribution is:

$$\gamma_0 = \frac{C_0}{\gamma_n T} = -2U \sum_k \frac{\partial f_k}{\partial T} \partial \psi \quad (19)$$

where ψ is replaced by $|\bar{\psi}|$ in the variational approach and by $\langle|\psi\rangle$ in the average value approach.

In practice, the amplitude specific heat can be calculated by using the entropy. C_0 is the derivative of the entropy times the temperature:

$$C_0 = -T \frac{\partial S}{\partial T} \quad (20)$$

where the entropy S for a fermionic system in the presence of a gap $|\psi|$ is a universal function of the ratio $|\psi|/T$:

$$S(|\psi|/T) = \sum_k f_k \log(f_k) \quad (21)$$

where the Fermi distribution is $f_k = \frac{1}{e^{-\beta(E_k - \mu)} + 1}$ and the energy E_k is $E_k = \sqrt{\xi_k^2 + |\psi|^2}$. By using the entropy, it is not necessary to perform the sum over k each time one wants to evaluate the specific heat. It is then sufficient to take the derivative of the entropy.

Normalisation of the specific heat: γ_0 is 1 at high temperature since it is divided by the Sommerfeld constant γ_n . The phase contribution is normalised as:

$$\frac{C_1}{\gamma_n} = \frac{k_B}{\xi_0^3 \gamma_n} \frac{C_\phi^{(s)}}{N k_B} \quad (22)$$

where C_1 is the specific heat per volume $V = N \xi_0^3$, and $C_\phi^{(s)}/(N k_B)$ is the specific heat per number of lattice sites coming from the simulations. Experiments give $\gamma_n \approx 26 \text{ mJ K}^{-1} \text{ mol}^{-1} = 252 \text{ J K}^{-1} \text{ m}^{-3}$. For the fit of Fig. 6, using the reasonable value $\xi_0 \approx 16 \text{ \AA}$, we get the dimensionless constant $\alpha = k_B/(\xi_0^3 \gamma_n) \approx 13.5$.

Doping	T_c [K]	V_0 [K]	T_0 [K]	α
0.92	92.9	261.9	124.3	13.7
0.87	93.7	178.0	143.3	14.3
0.80	88.8	121.8	158.9	10.6
0.73	69.3	111.0	177.6	13.7
0.67	60.8	88.9	193.0	18.1
0.57	55.9	76.1	213.5	20.6
0.48	47.7	57.6	241.5	16.0
0.43	31.5	37.3	251.2	9.0

TABLE I: Extracted parameters from the fits of YBCO specific heat. (see Figure 7).

A. Variational Method (d-wave)

Using the variational method the specific heat C is now

$$\gamma = \gamma_0 (|\bar{\psi}|) + \gamma_1 \quad (23)$$

where the amplitude $|\bar{\psi}|$ is now solution of the amplitude equation (10) The dimensionless constant is $\alpha \approx 13.5$.

In Fig. 6 the experimental specific heat of $\text{YBa}_2\text{Cu}_3\text{O}_{6.73}$ [1] is fitted using the variational method reproducing the double peak structure: a sharp peak below T_ϕ coming from phase fluctuations and a wide hump below T^* rounded by amplitude fluctuations. The crossover temperature T_ϕ , where phases become random, corresponds to the temperature where γ_1 is less than approximately 2% of the normal specific heat. In amplitude equation (10), a 2 dimensional density of states $D(\varepsilon) = 1/W$ is used with $W = 5000\text{K}$, $\mu = 0.25W$ and $U = 959\text{K}$. These parameters gives $T_0 \approx 200\text{K}$ and $\psi_0 \approx 2.14T_0$ in agreement with experiments [16]. The other parameters are $V_0 = 72\text{K}$ and $\eta = 5$.

B. Average Value Method (d-wave)

Following equation (16), the specific heat is given by

$$\gamma = \gamma_0 (\langle |\psi| \rangle_{GL}) + \gamma_1 \quad (24)$$

where γ_1 is divided by T_c instead of T since S_{GL} is a classical action and does not satisfy the Nernst theorem.

The average value method is compared to specific heat obtained for different doping in Fig. 7. For underdoped systems $x < 0.80$ we use simulations in $d = 2$. For the more overdoped, $x \geq 0.80$, simulations are done in $d = 3$. The parameter η is fixed to 3. Parameters V_0 and T_0 extracted from the fits are shown in the phase diagram of Fig. 14 and in table I. Values of the phase specific heat normalisation constant α range from 10 to 20. The fitting procedure is done completely automatically by a random walk in the parameter space $\{V_0, T_0, \alpha\}$, until the error between experimental data and the fit is minimal. As

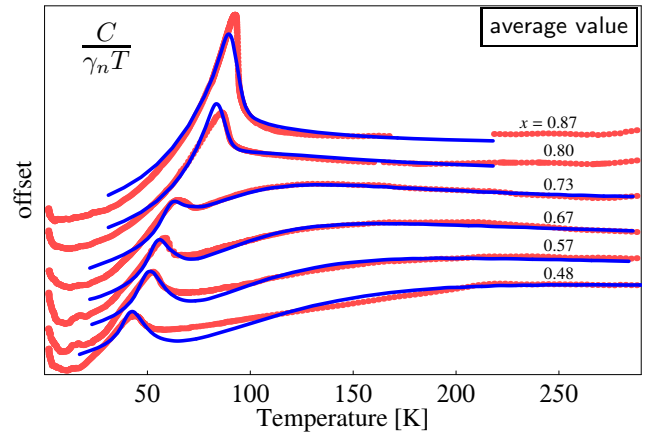


FIG. 7: $\text{YBa}_2\text{Cu}_3\text{O}_{6+x}$ specific heat for different oxygen dopings x compared to the average value method.

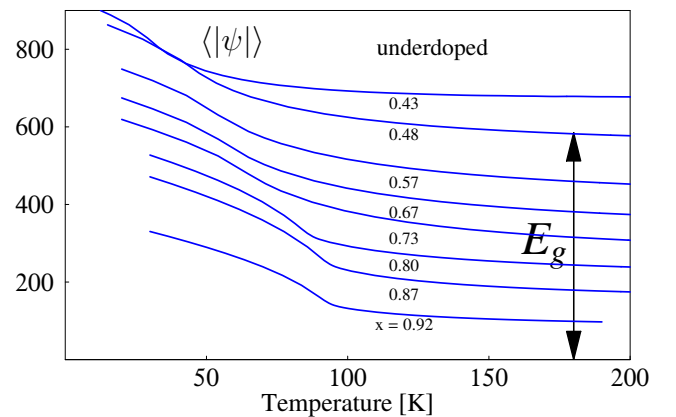


FIG. 8: Average amplitude corresponding to $\text{YBa}_2\text{Cu}_3\text{O}_{6+x}$ specific heat of Fig. 7 for different oxygen dopings x . The amplitude for maximum T_c resembles more to BCS behaviour whereas the amplitude for underdoped system is very large above T_c due to fluctuations and large T_0 .

usual, a local minimum can be reached by using this procedure, and one can be trapped in this minimum. However, when the dimension of the parameter space is 3 as in our case, different local minima can be easily excluded and the best fit can be achieved.

The temperature T_ϕ is derived from figure 9 where the average amplitude is compared to the average amplitude $\langle |\psi| \rangle_r$ computed for a field where phases are random, i.e. the gradient of phases is set to $\pi/2$:

$$\langle |\psi| \rangle_r = \frac{1}{Z_r} \int d|\psi| |\psi| |\psi| e^{-\frac{V_0}{T} [\eta^2 (t|\psi|^2 + \frac{1}{2}|\psi|^4) + D|\psi|^2]} \quad (25)$$

where D is the dimension of the system and the normalisation factor Z_r is

$$Z_r = \int d|\psi| |\psi| e^{-\frac{V_0}{T} [\eta^2 (t|\psi|^2 + \frac{1}{2}|\psi|^4) + D|\psi|^2]} \quad (26)$$

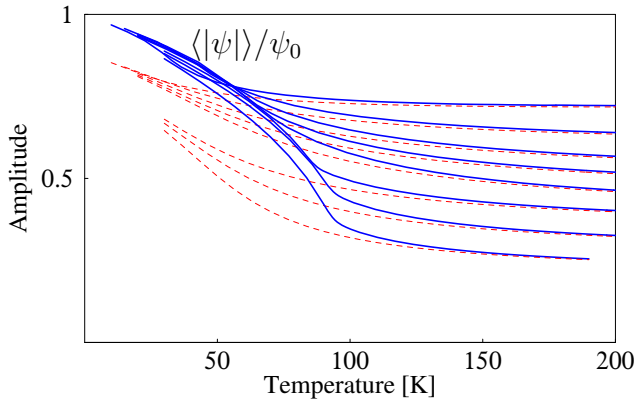


FIG. 9: Reduced average amplitude corresponding to $\text{YBa}_2\text{Cu}_3\text{O}_{6+x}$ specific heat for different oxygen dopings x . The dashed lines are average amplitudes calculated for a completely disordered phase field. Dopings are the same as in figure 8

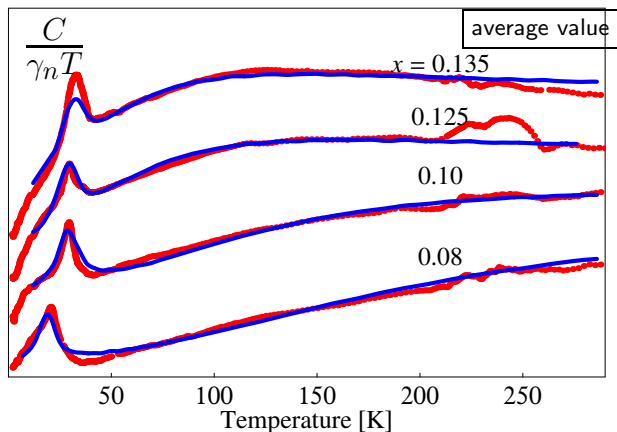


FIG. 10: Underdoped $\text{La}_{2-x}\text{Sr}_x\text{CuO}_4$ specific heat for different strontium dopings x compared to the d -wave average value method.

C. s -wave Symmetry

The measured **specific heat** of $\text{YBa}_2\text{Cu}_3\text{O}_{6.76}$ [1] is compared to our results for the s -wave symmetry in Fig. 11 by using the average value method.

We took the following values for the two parameters: $T_0 = 235\text{K}$ is of the order of T^* , $V_0 = 108\text{K}$ is of the order of T_c . For the size of ψ we took the BCS d -wave relation: $\psi(T=0) = 2.14T_0$ since it seems to be more in agreement with experiments [16] than the BCS relation of $\psi(T=0) = 1.76T_0$. This choice plays only a little quantitative role.

The mean amplitude, standard deviation and phase stiffness are presented in Fig. 12 for the same parameters as in Fig. 11. The coherence length ξ is of the order the lattice constant when the temperature T_ϕ is reached.

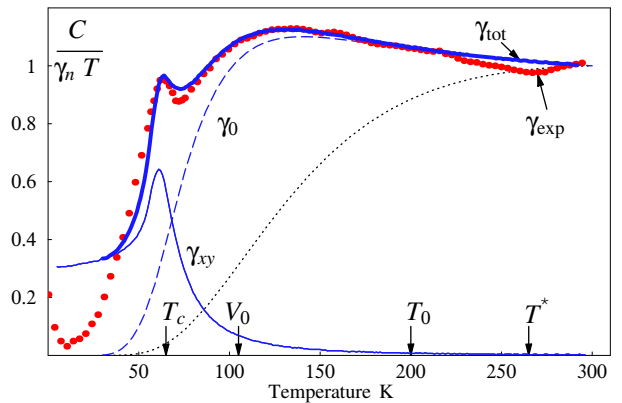


FIG. 11: Measurements (points) of the specific heat of $\text{YBa}_2\text{Cu}_3\text{O}_{6.76}$ divided by $\gamma_n T$. The total s -wave specific heat (thick blue) is the sum of the critical XY contribution (thin blue) and the amplitude contribution (dashed blue). If the amplitude of the gap were constant of size $2.14T_0$, the contri-

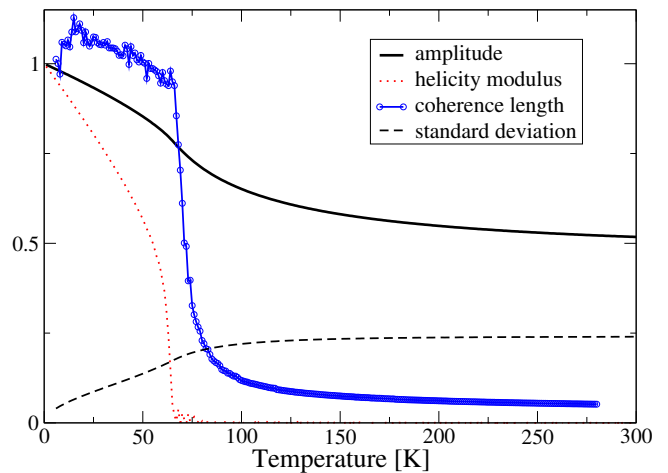


FIG. 12: The average amplitude $\langle |\tilde{\psi}| \rangle$ (thick) is large even above T_c whereas the coherence length ξ vanishes rapidly above T_c . The standard deviation $\sqrt{\langle |\psi|^2 \rangle - \langle |\tilde{\psi}| \rangle^2}$ (dashed line) is large and almost constant. The phase stiffness Γ_x in x direction (dotted red) jumps from $2/\pi$ to zero at T_c . Lattice size: $N = 80^2$. Parameters are $T_0 = 235\text{K}$, $V_0 = 108\text{K}$, $\eta^2 = 8$.

Considering Fig. 11, we see that an s -wave computation fits equally well experiments as the d -wave in Fig. 7. Hence, we cannot decide which symmetry is favored by looking at specific heat data. s -wave and d -wave symmetries are essentially different at low temperatures. d -wave specific heat has an algebraic increase with temperature whereas s -wave specific heat has an exponential behaviour. Therefore the s -wave contribution is smaller at low temperature than the d -wave. However, a lower s -wave contribution can be compensated by changing parameters T_0 and V_0 .

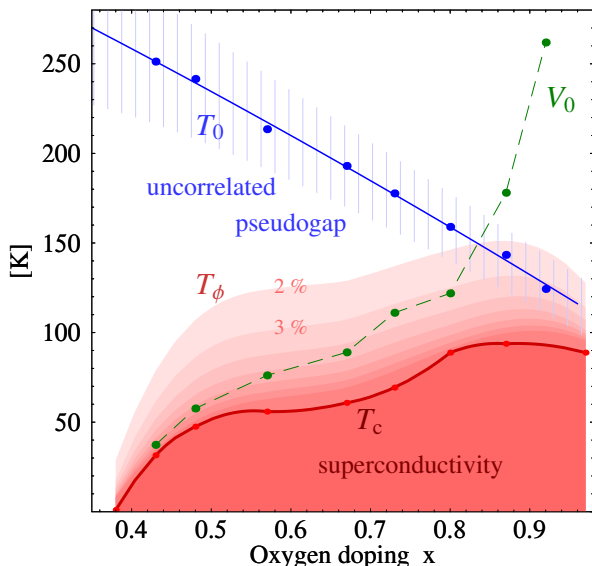


FIG. 13: Extracted phase diagram of $\text{YBa}_2\text{Cu}_3\text{O}_{6+x}$. Effects of amplitude fluctuations are large in the quasi uncorrelated pseudogap region (below T_0) of the copper oxides phase diagram, whereas phase correlations remain important only below T_ϕ . The temperature T^* , where observables cross over to normal behaviour, is located in the hatched area.

V. EXTRACTED PHASE DIAGRAM

Values for T_0 , V_0 and T_ϕ extracted for the specific heat in Fig. 7 are reported in Fig. 14. T_1 is the temperature where $C_\phi/\gamma_n = 2\%$. T_ϕ is computed in the same way as shown in Fig 2 but for average amplitudes used for specific heat fits. The energy scale E_g of the pseudogap is defined here as the amplitude at $T = 200\text{K}$: $E_g = \langle |\psi| \rangle_{T=200\text{K}}$. E_g shows the same doping dependence as the one found by Loram and Tallon [4]. However E_g is not due to some hidden critical point, but is related to the average amplitude in the pseudogap regime.

It is remarkable that phase correlations above T_c grow rapidly in the underdoped regime following the T_ϕ line, and reduce when approaching the overdoped regime. T_ϕ lines are similar to Nernst effect results [8], whereas the gradient specific heat seems to disappears more rapidly. This latter doping dependence is in better agreement with the phase diagram derived in Hall effect experiments [17].

VI. DIFFERENTIAL CONDUCTANCE

The differential conductance between a normal metal and a superconductor is directly related to the density of states and the amplitude of the pairing field by the

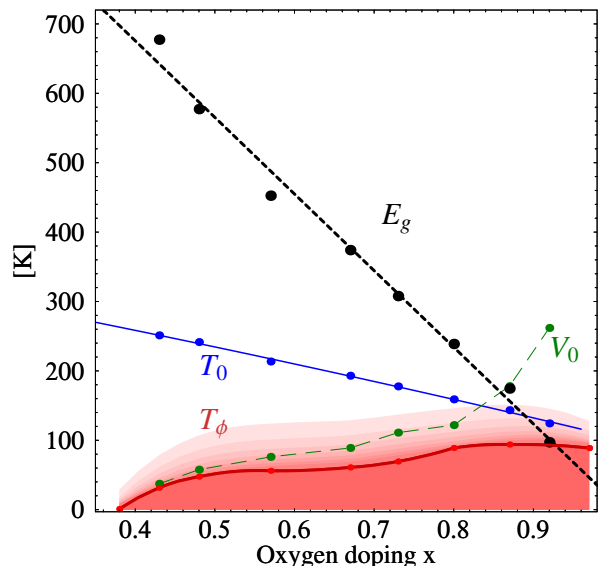


FIG. 14: The pseudogap energy scale E_g in the extracted phase diagram of $\text{YBa}_2\text{Cu}_3\text{O}_{6+x}$. Note that E_g is should only be zero if $T_0 = 0$, i.e. E_g is never zero in the superconducting regime so that there is no quantum critical point hidden by superconductivity.

standard formula:

$$\frac{dI}{dV} = -G_{nn} \sim \frac{N_s(\xi)}{N(0)} \frac{\partial f(\xi + eV)}{\partial(eV)} \quad (27)$$

where G_{nn} is the differential conductance between two normal metals. The reduced energy is $\xi = \varepsilon - \mu$. The s -wave density of states is according to BCS theory:

$$N_s(\xi) = |\xi| / \sqrt{\xi^2 - \langle |\psi| \rangle^2} \quad (28)$$

Of course, $N_s(\xi) = 0$ if $|\xi| < \langle |\psi| \rangle$.

In Fig. 15, the s -wave differential conductance normalised with G_{nn} is presented using the same parameters as in Fig. ?? for temperatures from 20 K to 300 K with 40 K intervals. One can see that the width of the differential conductance is proportionnal to the amplitude $\langle |\psi| \rangle$, and that the gap fills up due to thermal energy. The low temperature differential conductance at $V = 0$ is approximately given by [18]:

$$\frac{dI}{dV}(V=0) \approx G_{nn} \sqrt{\frac{2\pi|\psi|}{T}} e^{-|\psi|/T} \quad (29)$$

Theses results are in agreement with scanning tunneling microscopy on $\text{Bi}_2\text{Sr}_2\text{CaCu}_2\text{O}_8$ of Renner *et al* [19] where it is observed that the pseudogap gradually fills up whereas its width remains constant. Do phase fluctuations contribute to the pseudogap? Yes but only up to V_0 where the coherence length ξ is of the order of the lattice spacing as seen in Fig. 12. As shown by Eckl *et al* [20], an amplitude of size $2T_0$ maintains a pseudogap in the density of states up to T^* whereas phase effects disappear near T_c .

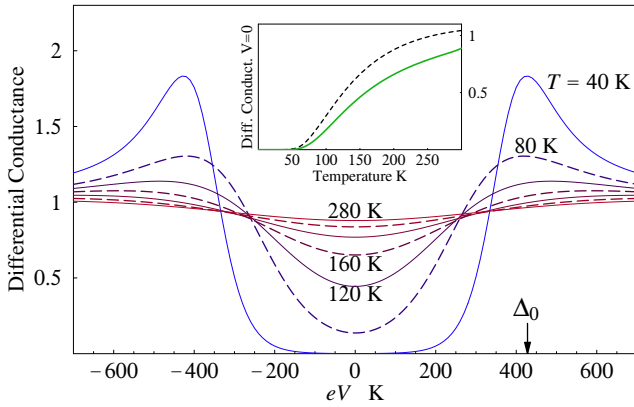


FIG. 15: The differential conductance of equation (27) shows a pseudogap, i.e a partial suppression of the density of states, up to temperatures near $T^* \approx 300$. Inset: the differential conductance (green curve) at $V = 0$ recovers its normal behaviour near T^* . The low temperature approximation of equation (29) is shown by the dashed line.

VII. DISCUSSION

We have shown that amplitude and phase fluctuations can explain the emergence of the pseudogap region of underdoped high temperature superconductors. Phase coherence disappears completely near a temperature T_ϕ above T_c , and therefore, for $T > T_\phi$, the pseudogap region is dominated by amplitude fluctuations. We find that the mean field temperature T_0 has a similar doping dependence as T^* , signaling that the pseudogap region is due to independent fluctuating pairs. The energy scale E_g of the pseudogap is also derived. The large value of E_g in the underdoped domain is due to a finite T_0 and large amplitude fluctuations. At maximum doping, T_0

remains of the order of T_c but amplitude fluctuations are much weaker. Therefore E_g vanishes linearly when approaching maximum doping. The fact that E_g takes small values above maximum doping should not be interpreted as a quantum critical point since fluctuations survive in the overdoped regime as well: E_g has always a finite value because of amplitude fluctuations.

Comparison with measured specific heat on underdoped LSCO reproduces the double peak structure like in YBCO: a sharp peak below T_ϕ coming from phase fluctuations and a separate wide hump below T^* rounded by the amplitude. The spin susceptibility, related to the amplitude, recovers its normal behaviour near T^* whereas the orbital magnetic susceptibility, related to phases, disappears near T_ϕ . These considerations are independent of the underlying pairing mechanism, and any microscopic theory inducing pairing should lead to similar conclusions.

An important difference between overdoped and underdoped superconductors is the "separation" between effects due to amplitudes and phases: in the overdoped regime, contributions of amplitude and phase are added producing only one peak in the specific heat for example. In the underdoped regime, phase correlations remain near T_c and still produce a small peak whereas amplitude fluctuations extend to much larger temperature producing a separate wide hump between T_c and T^* .

Further work is needed in order to include in the theory effects of the magnetic field on the pseudogap.

This work has been supported by the Swiss National Science Foundation.

-
- [1] J. W. Loram, K. A. Mirza, J. M. Wade, J. R. Cooper and W. Y. Liang, *Physica C* **134**, 235 (1994).
 - [2] T. Timusk and S. Bryan, *Rep. Prog. Phys.* **62**, 61 (1999).
 - [3] S. Sachdev, *Quantum Phase Transition* (Physics World, 1999).
 - [4] J. Tallon and J. Loram, 2000, cond-mat/0005063.
 - [5] V. J. Emery and S. A. Kivelson, *Nature* **374**, 4337 (1995).
 - [6] Z. A. Xu, N. P. Ong, Y. Wang, T. Kekeshita and S. Ushida, **406**, 486 (2000).
 - [7] P. Curty and H. Beck, *Phys. Rev. Lett.* **91**, 257002 (2003).
 - [8] Y. Wang *et al.*, *Phys. Rev. B* **64**, 224519 (2001).
 - [9] M. Takigawa, *et al.*, *Phys. Rev. B* **43**, 247 (1991).
 - [10] P. Pieri *et al.*, *Phys. Rev. Lett.* **89**, 127003 (2002).
 - [11] P. Devillard *et al.*, *Phys. Rev. Lett.* **84**, 5200 (2000).
 - [12] B. L. Gyorffy *et al.*, *Phys. Rev. B* **44**, 5190 (1991).
 - [13] P. Curty and H. Beck, *Phys. Rev. Lett.* **85**, 796 (2000).
 - [14] U. Wolff, *Phys. Rev. Lett.* **62**, 361 (1989).
 - [15] R. C. Brower and P. Tamayo, *Phys. Rev. Lett.* **62**, 1087 (1989).
 - [16] M. Kugler *et al.*, *Phys. Rev. Lett.* **86**, 4911 (2001).
 - [17] D. Matthey *et al.*, *Phys. Rev. B* **64**, 24513 (2001).
 - [18] M. Tinkham, *Introduction to Superconductivity* (McGraw-Hill, 1996).
 - [19] Ch. Renner *et al.*, *Phys. Rev. Lett.* **80**, 149 (1997).
 - [20] T. Eckl, 2001, cond-mat/0110377.